Leakage and counting errors in a seven-junction electron pump

R. L. Kautz, Mark W. Keller, and John M. Martinis

National Institute of Standards and Technology, 325 Broadway, Boulder, Colorado 80303

Leakage and counting errors are explored experimentally in a well-characterized seven-junction electron pump and compared with predictions of the orthodox theory, including cotunneling. Theory and experiment are in good agreement at intermediate temperatures, where errors are dominated by thermally activated, single-junction processes. At low temperatures, however, the observed errors far exceed predictions, indicating that the orthodox theory omits an important error process.

[S0163-1829(99)03135-5]

I. INTRODUCTION

In 1991 Pothier *et al.*[1] first demonstrated a circuit, based on the Coulomb blockade in nanoscale tunnel junctions, that transfers a single electron between input and output in response to each cycle of an applied bias sequence. Called an electron pump, the device has potential applications in fundamental metrology as a standard of either current[1] or capacitance,[2] provided that it can count electrons with high accuracy. Initial tests established a counting accuracy of 0.1% for a three-junction pump,[1] and later tests of five- and seven-junction pumps demonstrated accuracies of 500 parts per 10^9 and 15 parts per 10^9, respectively.[3,4] While the seven-junction pump is accurate enough for many metrological applications, the observed error rate is many orders of magnitude higher than that predicted for the nominal operating temperature. Early tests led to the conclusion that either the temperature of the pump is significantly higher than that of the dilution refrigerator used to cool it or an important error mechanism has been omitted from the theoretical analysis. Further experiments, outlined recently,[5] measured the pump temperature directly and showed that the observed error rates are clearly inconsistent with the predictions of the ''orthodox'' theory,[6] with cotunneling added. Here, we present a more detailed comparison of theory and experiment for two types of errors, associated with counting and leakage, in a well-characterized seven-junction electron pump.

With regard to errors in counting, we consider two different measures. The simplest measure is the net charge error, $\mathcal{E}_Q = ||Q|/e - 1|$, or the absolute difference between the average charge Q and expected charge e transferred during a pump cycle. $\mathcal{E}_Q$ is a direct measure of the accuracy of an electron pump used as a current standard and has been calculated by several authors for a variety of situations.[7-12] However, the most stringent experimental tests of pump accuracy have recorded the infrequent error events, whether positive or negative, occurring while the pump is used to shuttle one or two electrons repeatedly back and forth.[3,4] The shuttle test records an error either if extra electrons are transferred or if there is an electron deficit during a pump cycle. The shuttle error can be expressed as $\mathcal{E}_S = (Q_+ + Q_-)/e$, where $Q_+ \geq 0$ is the average extra charge transferred and $Q_- \geq 0$ is the average deficit. In these terms, the net charge error is $\mathcal{E}_Q = |Q_+ - Q_-|/e$, so $\mathcal{E}_S$ is an upper bound on $\mathcal{E}_Q$.

Indeed, the bias voltage across the pump can be adjusted to produce a cancellation between positive and negative errors that yields $\mathcal{E}_Q = 0$, but the shuttle error is never zero. In this paper, we focus on the shuttle error to facilitate comparison with experimental shuttle-error measurements.

The second type of error to be considered is the leakage rate of the pump when biased in its hold mode. Such errors are relevant to the capacitance standard, in which a pump is used to charge a capacitor and then put in the hold mode while the capacitor's voltage is measured. In a capacitance standard, the leakage rate must be small to insure that the charge on the capacitor remains constant during the voltage measurement. Because the hold mode requires fixed biases, leakage in the pump is simply leakage in the Coulomb blockade of a series array of junctions, and this leakage has been measured experimentally both for its intrinsic interest[13,14] and in the context of the pump.[3,4,15] Strategies for calculating the net leakage current I_L, including cotunneling, have been developed by several authors.[8,16-18] However, as with pumping errors, the most sensitive measurements of leakage observe the tunneling of single electrons and record the mean time between tunneling events, whether in the forward or reverse direction. If we define $I_+ \geq 0$ and $I_- \geq 0$ as the average currents associated with tunneling in the forward and reverse directions, it is useful to examine the absolute leakage current $I_A = I_+ + I_-$, as well as the net leakage current $I_L = I_+ - I_-$. The absolute leakage current is more relevant than I_L in single-electron experiments because I_A is related to the mean time between leakage events by $\tau_L = e/I_A$. Thus, I_A determines the time allowed for measuring the capacitor's voltage when a pump is used in a capacitance calibration.

In this paper, we consider three circuit models for the electron pump. As shown in Fig. 1(a), a pump consists of $N \geq 3$ tunnel junctions connected in series. Here, the junctions are assumed to be identical and are characterized by the same capacitance C_J and tunnel resistance R_J. The $N-1$ islands between the junctions are biased by voltage sources V_i through identical gate capacitors C_g. The voltage sources can be independently controlled to sequence a single electron through the array to charge or discharge an external capacitor C_E. Because C_E is generally much larger than either C_J or C_g, we can replace C_E by a voltage source V_E in calculating error rates. If we also replace the series combinations of voltage source and gate capacitor by their Norton equivalents
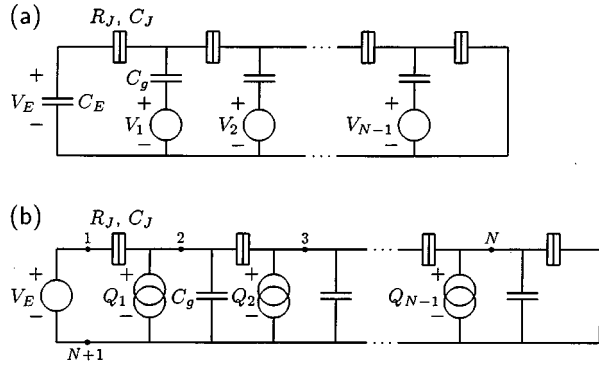
FIG. 1. Circuit diagrams of the electron pump representing the physical pump (a) and an equivalent circuit (b). Nanoscale tunnel junctions are indicated by boxes. Stray capacitances are not shown.

FIG. 2. Experimental record of charge on the external capacitor as a function of time for a seven-junction pump in the hold mode. The pump temperature is 120 mK, and the central junction of the pump is biased with a charge of $Q_{J4}=0.45\,e$.

of a charge source $Q_i=C_gV_i$ with a shunt capacitor C_g,[8] then we arrive at the equivalent circuit shown in Fig. 1(b). This equivalent circuit defines the ''ground capacitance'' or C_g model of the electron pump, given the understanding that C_J and C_g are parameters that can be adjusted to include the effects of stray capacitance. While the C_g model is the primary model considered in this paper, we also examine a simplified ''bare'' model, in which $C_g=0$, and a more complete ''full'' model, which includes stray capacitances between all possible pairs of the $N+1$ nodes in Fig. 1(b). For the seven-junction pump discussed here, the bare model is inadequate to explain some qualitative features of the pump, while the C_g model produces results nearly identical to those of the full model.

The calculations in this paper use orthodox theory,[6] with cotunneling added, to determine error rates for a seven-junction pump that was carefully characterized experimentally. As noted previously,[5] our primary result is that the predicted and observed error rates are in rough agreement at high temperatures, where thermal activation is the dominant error mechanism, but may differ by almost nineteen orders of magnitude at low temperatures, where cotunneling is dominant. Because the temperature and circuit parameters of the pump are well known, an additional error mechanism, such as cosmic ray excitation[5] or photon-assisted tunneling produced by environmental noise[19] or the cyclic bias,[20] is required to explain the errors observed in the low-temperature regime. This is an important conclusion both because the pump is most accurate and of greatest utility at low temperatures and because it indicates that the physics of the pump is not entirely understood. We now present detailed evidence supporting our conclusion, considering first leakage and then counting errors.

II. LEAKAGE

When biased in the hold mode, the junctions of a pump present a static energy barrier that can be traversed by electrons only through thermal activation or multijunction tunneling. These processes allow an occasional electron to leak through the pump, changing the charge on the external capacitor by e. When the charge on C_E is monitored using an electrometer, we typically obtain a record of a discrete random walk, like that shown in Fig. 2. In this instance, the charge jumps suddenly by $\pm e$ at intervals on the order of 1 s, in an apparently random fashion. As noted above, the average time τ_L between such jumps determines the absolute leakage current $I_A=e/\tau_L$, a useful measure of the leakage rate.
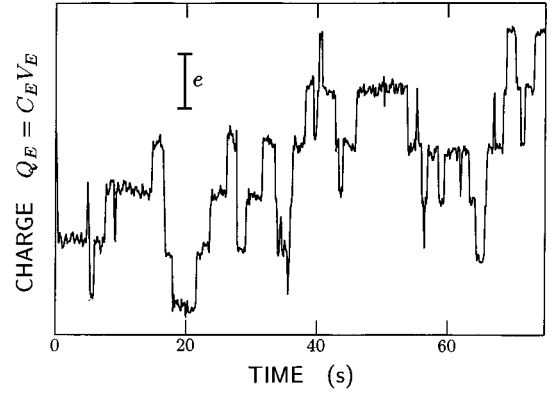
A. Theory

In order to compare experiment and theory, which is essential to this study, we calculate the leakage rate using a procedure developed by Jensen and Martinis,[8] as modified by Fonseca *et al.*[17] This procedure is based on the orthodox theory of single-electron tunneling[6] and incorporates multijunction cotunneling processes using an approximation to the transition-rate formula developed by Averin and Odintsov.[16] While not entirely rigorous, various tests indicate that the procedure is usually reliable for order-of-magnitude estimates.[8]

Calculation of the leakage current I_L is formulated in terms of the probabilities P_n that the pump is in a charge state n and the rates $\Gamma_{n'n}$ of transitions between states n and n'. Here, the index n specifies the charge on each of the $N-1$ islands of the pump. Thus, if the charge on each island is assumed to be between $-Me$ and Me, the index n must take on a total of $(2M+1)^{N-1}$ values to specify all possible charge states. The probabilities of the various charge states evolve according to

$$\frac{dP_n}{dt}=\sum_{n'\neq n}(\Gamma_{nn'}P_{n'}-\Gamma_{n'n}P_n),\qquad(1)$$

where the first term accounts for the increase in P_n due to transitions from n' to n and the second term accounts for the decrease due to transitions from n to n'. In this transition-state picture, the ensemble average of the current through junction J at any instant is

$$I_J=e\sum_{n,n'}P_n[\Gamma_{n'n}^+(J)-\Gamma_{n'n}^-(J)],\qquad(2)$$

where the $\Gamma^+_{n'n}(J)$ are the rates of transitions in which a charge moves in the positive direction through junction J and the $\Gamma^-_{n'n}(J)$ are the rates of transitions in which a charge moves in the negative direction through junction J.

The net leakage current is particularly simple to calculate because the biases are fixed in the hold mode, and the pump quickly approaches a steady state. Thus, the relevant probabilities are defined by the steady-state conditions

$$\frac{dP_n}{dt}=0, \tag{3}$$

and I_L can be evaluated by applying Eq. (2) to any junction of the pump. On the other hand, there is no simple formula for the absolute leakage current, and, as discussed below, care must be exercised in identifying which terms in Eq. (2) contribute to I_A.

Equations (1)–(3) allow us to solve for the steady-state probabilities and currents provided the rates $\Gamma_{n'n}$ can be calculated. In general, $\Gamma_{n'n}$ includes contributions from an infinite number of processes that take the system from charge state n to n'. All multijunction cotunneling processes can be broken into a sequence of single-junction tunneling events, and, following Jensen and Martinis,[8] we specify a process by a list of integers $(j_1, j_2, \ldots, j_m)$. Here, each j_i is a number in the range $\pm 1, \pm 2, \ldots, \pm N$, which specifies the junction and the direction of tunneling for each event in the sequence. The process $(j_1, j_2, \ldots, j_m)$ is said to be an mth-order process because m single-junction events are included. Schematically, a third-order process for a transition from charge state n to n' can be diagrammed as follows.

event: j_1 j_2 j_3

state: $n \quad \rightarrow \quad s_1 \quad \rightarrow \quad s_2 \quad \rightarrow \quad n'$

$\quad\quad\quad \delta E_1 \quad\quad \delta E_2 \quad\quad \delta E_3$

energy: $0 \quad\quad \Delta E_1 \quad\quad \Delta E_2 \quad\quad \Delta E_3$ (4)

In this representation, we associate a change in Coulomb energy δE_i with the ith tunneling event and a net change in Coulomb energy $\Delta E_i = \sum_{j=1}^{i} \delta E_j$ with the partially completed process. These Coulomb energies determine the energy barrier for multijunction cotunneling and are the primary factors fixing the associated transition rate. The δE_i can be computed from the electrostatics of the pump's capacitance network, given the initial and final charge states.

Because the order of the single-junction tunneling events $(j_1, \ldots, j_m)$ does not affect the final state, all $m!$ permutations of the set $\{j_1, \ldots, j_m\}$ contribute to the rate of transition from n to n'. In the approximation of Jensen and Martinis,[8] the contribution to the transition rate from this set of mth-order processes is

$$\Gamma^{(m)}_{n'n}=\frac{2\pi}{\hbar}\left[\frac{R_K}{(2\pi)^2 R_J}\right]^m S^2 F_m(\Delta E_m, T), \tag{5}$$

where $R_K = h/e^2$ is the resistance quantum,

$$S=\sum_{\text{perm}\{j_1,\ldots,j_m\}}\prod_{i=1}^{m-1}\left(\Delta\tilde{E}_i-\frac{i}{m}\Delta E_m\right)^{-1}, \tag{6}$$

and

$$F_m(\Delta E_m, T)=\frac{-\Delta E_m/(2m-1)!}{1-\exp(\Delta E_m/k_B T)}$$
$$\times\prod_{i=1}^{m-1}[(2\pi i k_B T)^2+(\Delta E_m)^2]. \tag{7}$$

In the original derivation of Eq. (6), the energy $\Delta\tilde{E}_i$ is simply ΔE_i, but in this case S is dominated by an unphysical singularity whenever an intermediate ΔE_i falls on or near the interval between 0 and ΔE_m. Jensen and Martinis handled such singularities by omitting processes that include a ΔE_i less than $\max(0, \Delta E_m)$. In order to eliminate the resulting discontinuities in $\Gamma_{n'n}$, Fonseca et al. later suggested that $\Delta\tilde{E}_i$ be held fixed within a buffer zone of width $k_B T$ around the singular interval.[17] Here, we adopt a similar strategy by assuming that

$$\Delta\tilde{E}_i=\max(\Delta E_i, k_B T, \Delta E_m+k_B T), \tag{8}$$

which produces rates essentially identical to those of Fonseca et al.

Equations (5)–(8) completely specify an approximate rate for all mth-order processes involving the set $\{j_1, \ldots, j_m\}$ of single-junction events, regardless of order. If we define the unordered set $\{j_1, \ldots, j_m\}$ as a configuration, then the only additional approximation to be made is that of selecting a finite number of configurations that includes all processes contributing significantly to the dynamics of the pump. In this selection, we follow Jensen and Martinis by eliminating configurations of order $m > N$, configurations in which tunneling occurs more than once in a given junction, and configurations that involve tunneling in both the forward and reverse directions. With these restrictions, the total number of configurations to be considered is

$$N_C=2\sum_{m=1}^{N}\frac{N!}{m!(N-m)!}=2^{N+1}-2, \tag{9}$$

or 254 configurations for a seven-junction pump. The rate matrix $\Gamma_{n'n}$ is computed by summing the contributions due to each process within each tunneling configuration acting on each initial state n. Since we also restrict the charge on a given island to the range between $-Me$ and Me, processes that lead at any point to a junction charge outside of this range are omitted from the sum.

Once $\Gamma_{n'n}$ has been evaluated, Eqs. (1)–(3) can be solved for the steady-state probabilities P_n and the net leakage current I_L. While it might be assumed that the absolute leakage current I_A can be calculated simply by replacing $\Gamma^+_{n'n} - \Gamma^-_{n'n}$ with $\Gamma^+_{n'n} + \Gamma^-_{n'n}$ in Eq. (2), this strategy fails because it includes many processes that do not involve the transfer of a charge through the entire pump. Instead, I_A must be evaluated by explicitly adding contributions from combinations of cotunneling processes that produce a through transfer. Within the approximation used here, a through transfer requires N single-junction tunneling events, one for each junc-

tion, but these can be distributed arbitrarily among several cotunneling processes. Suppose that a through transfer in the forward direction consists of K cotunneling processes that take the pump from an initial state n_0 through the successive states $n_1, \ldots, n_K$, where the final state n_K necessarily coincides with the initial state. To calculate the rate for this transfer, we note first that the rate of transitions from n_0 to n_1 is $P_{n_0}\Gamma^+_{n_1 n_0}$, where $\Gamma^+_{n'n}$ is the rate for forward tunneling processes only ($\Gamma_{n'n} = \Gamma^+_{n'n} + \Gamma^-_{n'n}$). Next, we argue that, under steady-state conditions and given that the pump is already in state n_1, the probability of a transition from n_1 to n_2 is the rate $\Gamma^+_{n_2 n_1}$ divided by the total rate $\Gamma_T(n_1) = \Sigma_{n' \neq n_1}\Gamma_{n'n_1}$ for leaving state n_1. Thus, the rate of transitions from n_0 to n_1 to n_2 is $P_{n_0}\Gamma^+_{n_1 n_0}\Gamma^+_{n_2 n_1}/\Gamma_T(n_1)$. Multiplying this result by the probabilities for the remaining transitions leads to the rate $P_{n_0}\Gamma^+_{n_1 n_0}\Pi^K_{j=2}[\Gamma^+_{n_j n_{j-1}}/\Gamma_T(n_{j-1})]$ for the entire through transfer. Based on these arguments, the leakage currents in the forward and reverse directions can be written as

$$I_\pm = e \sum_{\substack{\text{through} \\ \text{transfers}}} P_{n_0}\Gamma^\pm_{n_1 n_0}\prod_{j=2}^K \frac{\Gamma^\pm_{n_j n_{j-1}}}{\Gamma_T(n_{j-1})}, \quad (10)$$

with

$$\Gamma_T(n) = \sum_{n' \neq n}\Gamma_{n'n}, \quad (11)$$

where the product is understood to be 1 when $K=1$. In Eq. (10), the specified sum over through transfers includes values of K from 1 to N, allowing transfers ranging from a single N-junction cotunneling process to N separate single-junction processes. Also, for a given K, the single-junction events must be distributed in all possible ways among the K cotunneling processes. Finally, the sum includes all initial states n_0, but, to avoid double counting, terms are only included if the probabilities of all intermediate states, $n_1, \ldots, n_{K-1}$, are less than P_{n_0}. This restriction is necessary because the states of a through transfer form a cycle, $n_0 \to n_1 \cdots \to n_{K-1} \to n_0$, and only one state can be chosen as the initial/final state. Thus, while evaluation of the absolute leakage current $I_A = I_+ + I_-$ is somewhat complicated, the only data required are the steady-state probabilities P_n and the rate matrices $\Gamma^+_{n'n}$ and $\Gamma^-_{n'n}$ for forward and reverse tunneling.

To illustrate the distinction between the net and absolute leakage currents, we plot $|I_L| = |I_+ - I_-|$ and $I_A = I_+ + I_-$ as a function of the bias voltage V_E in Fig. 3 for a seven-junction pump at 25 mK. For bias voltages greater than about 5 μV in magnitude, the current is dominated by leakage in either one direction or the other, and $|I_L| \approx I_A$. At $V_E = 0$, on the other hand, leakage is equally likely in both directions, so $I_+ = I_-$, $I_L = 0$, and $I_A = 2I_+$. Thus, in contrast to I_L, the minimum value of I_A is nonzero and provides a useful measure of the minimum error rate of a pump in its hold mode. The quantity $I_A(V_E = 0)$ is also easily measured experimentally because the voltage on C_E automatically settles to the value for which $I_+ = I_-$, as illustrated in Fig. 2, and the resulting V_E is presumably near zero. In the remainder of this section, we thus focus on the absolute leakage current at zero voltage bias.
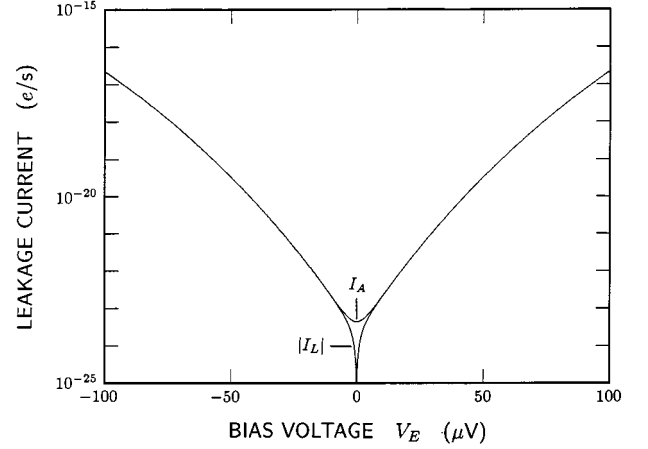
FIG. 3. Net leakage current I_L and absolute leakage current I_A as a function of the pump bias voltage V_E for a seven-junction pump at 25 mK, computed within the C_g model. The circuit parameters are $R_J = 470$ kΩ, $C_J = 220$ aF, and $C_g = 50$ aF. All gate charge biases are zero.

B. Asymptotic formulas

While leakage rates can be determined for the general case only numerically, the bare model possesses sufficient symmetry that asymptotic formulas can be derived in two low-temperature limits. Both formulas require that the thermal energy be much less than the basic Coulomb energy, $k_B T \ll E_C = e^2/2C_J$, and their regions of validity are separated by a crossover temperature $T_c \ll E_C/k_B$. In the extreme low-temperature limit, $T \ll T_c$, thermal processes play no significant role, and leakage occurs only by Nth-order cotunneling, in which all N junctions are traversed in one tunneling event. In the intermediate temperature range, $T_c \ll T \ll E_C/k_B$, thermal processes are dominant, and leakage occurs primarily through a sequence of N single-junction tunneling processes.

A simple analysis of the bare model is possible because the energy changes δE_i and ΔE_i in a through transfer are independent of the order in which the junctions tunnel when each junction participates exactly once. As shown by Jensen and Martinis,[8] these energies are given by

$$\delta E_i = E_C(N - 2i + 1)/N, \quad \Delta E_i = E_C i(N-i)/N, \quad (12)$$

in the absence of initial island charges and voltage or charge biases. The absolute leakage current for $T \ll T_c$ then follows directly from Eqs. (5)–(8), since we expect leakage to occur only by Nth-order cotunneling in this limit. That is, if we consider Eq. (10) and assume that the initial state n_0 is always the zero-charge state ($P_{n_0} = 1$) and that through transfers occur only by Nth-order cotunneling processes, then the absolute leakage current is given by $I_A = 2e\Gamma^{(N)+}_{n_0 n_0}$, where we have used the fact that forward and reverse tunneling rates are equal by symmetry. Without further approximation, $\Gamma^{(N)+}_{n_0 n_0}$ can be evaluated from Eqs. (5)–(8) using the above δE_i and ΔE_i to yield

$$I_A = \frac{2ek_BTN^2}{h(2N-1)!} \left(\frac{R_K}{R_J}\right)^N \left(\frac{Nk_BT}{E_C}\right)^{2N-2},$$

$$(T \ll T_c, \quad V_E = Q_i = 0). \qquad (13)$$

Because electron pumps are typically operated in this low-temperature limit, the above equation specifies the minimum leakage rate that can be expected under ideal conditions.

A formula for I_A at intermediate temperatures, $T_c \ll T \ll E_C/k_B$, is obtained by detailed analysis of Eq. (10), assuming that leakage is dominated by through transfers involving N single-junction or first-order tunneling processes. Thus, we consider only the case $K = N$ in Eq. (10) and again assume that the initial state is the zero-charge state. Because the energies δE_i and ΔE_i are the same, regardless of the order in which the junctions tunnel, the sum over through transfers in Eq. (10) is $N!$ times the rate for a given process. Finally, adding the equal contributions from forward and reverse tunneling, we obtain

$$I_A = 2eN! \Gamma^{(1)+}_{n_1 n_0} \prod_{j=2}^{N} \frac{\Gamma^{(1)+}_{n_j n_{j-1}}}{\sum_n \Gamma^{(1)}_{n n_{j-1}}}, \qquad (14)$$

where the intermediate states correspond to any one of the $N!$ equivalent through transfers.

In order to explicitly evaluate Eq. (14), we note that, according to Eqs. (5)–(8), the rate for a first-order process is

$$\Gamma^{(1)} = \frac{-\delta E/e^2 R_J}{1 - \exp(\delta E/k_B T)}, \qquad (15)$$

which can be usefully approximated in various regimes by

$$\Gamma^{(1)} = \begin{cases} \dfrac{|\delta E|}{e^2 R_J} & (\delta E < 0, \ |\delta E| \gg k_B T) \\[2ex] \dfrac{k_B T}{e^2 R_J} & (\delta E = 0) \\[2ex] \dfrac{\delta E}{e^2 R_J} \exp(-\delta E/k_B T) & (\delta E \gg k_B T) \end{cases} \qquad (16)$$

The task that remains is to combine these approximate rates to evaluate all of the factors appearing in Eq. (14). This task is facilitated by Fig. 4, which plots the energies ΔE_i of intermediate states for pumps with even ($N=4$) and odd ($N=5$) numbers of junctions. For a four-junction pump, δE is positive for the first two tunneling events (j_1 and j_2) and negative for the final two (j_3 and j_4), so the rates $\Gamma^{(1)+}$ appearing in the numerator of Eq. (14) can be approximated by the expressions for either $\delta E < 0$ or $\delta E > 0$ in Eq. (16). For a pump with an odd number of junctions, on the other hand, the middle tunneling event (j_3 for $N=5$) requires the rate for $\delta E = 0$. In both even and odd cases, the sums appearing in the denominator of Eq. (14) are dominated by terms with $\delta E < 0$, since the primary way of leaving a given state is always "downhill." Thus, the first denominator in Eq. (14) can be approximated by the rate of transitions from state n_1 to state n_0, the reverse of the initial j_1 tunneling event. Similarly, the second denominator can be approximated by the
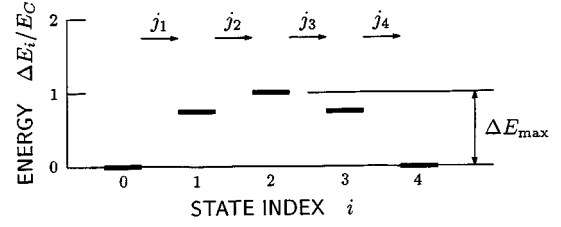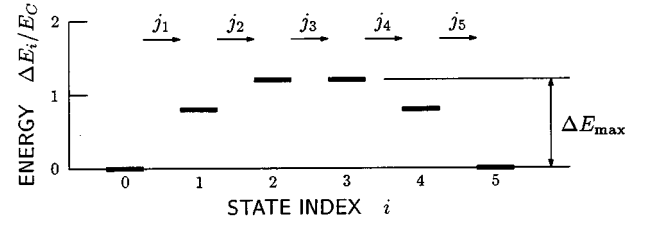
FIG. 4. Energy of intermediate states of a through tunneling process within the bare model of a four-junction (a) and a five-junction (b) electron pump. Energies are normalized to the basic Coulomb energy $E_C = e^2/2C_J$.

rate of reverse tunneling from state n_2, but in this case we must include two equal terms because either j_1 or j_2 can be reversed. Based on such considerations, we arrive at the following approximate formula for the absolute leakage current.

$$I_A = \begin{cases} \dfrac{N!}{2[(N/2)!]^2} \dfrac{E_C}{e R_J} \exp(-\Delta E_{\max}/k_B T) & (N \text{ even}) \\[3ex] \dfrac{2N!}{\{[(N-1)/2]!\}^2} \dfrac{k_B T}{e R_J} \exp(-\Delta E_{\max}/k_B T) & (N \text{ odd}) \end{cases} . \qquad (17)$$

Here the energy $\Delta E_{\max}$ is the barrier energy of the Coulomb blockade (cf. Fig. 4), which is given by

$$\Delta E_{\max} = \begin{cases} N E_C/4 & (N \text{ even}) \\ (N^2-1)E_C/4N & (N \text{ odd}) \end{cases}, \qquad (18)$$

within the bare model. Equation (17) is valid for $V_E = Q_i = 0$ in the temperature range $T_c \ll T \ll E_C/k_B$ and provides a useful check on numerical evaluations of I_A. As expected, I_A is thermally activated in this regime, with an activation energy equal to the pump's Coulomb barrier.

The crossover temperature T_c, defining the transition between the dominance of Nth-order cotunneling and that of single-junction processes, can be calculated by equating the expressions for I_A given in Eqs. (13) and (17). For an even number of junctions, we find

$$T_c = \frac{N E_C}{4 \alpha k_B}, \qquad (N \text{ even}) \qquad (19)$$

where α is defined by

$$\exp(\alpha) = \frac{2^{4N-4}N!(2N-1)!}{N^{4N-1}[(N/2)!]^2}\left(\frac{R_J}{R_K}\right)^{N-1}\alpha^{2N-1}, \quad (N \text{ even}) \tag{20}$$

while for N odd,

$$T_c = \frac{(N^2-1)E_C}{4N\alpha k_B}, \quad (N \text{ odd}) \tag{21}$$

with

$$\exp(\alpha) = \frac{N!(2N-1)!}{\{N[(N-1)/2]!\}^2}\left(\frac{4}{N^2-1}\right)^{2N-2}$$
$$\times \left(\frac{R_J}{R_K}\right)^{N-1}\alpha^{2N-2} \quad (N \text{ odd}) . \tag{22}$$

Although Eqs. (20) and (22) must be solved iteratively for α, these expressions allow a direct evaluation of the crossover temperature.

C. Model parameters

Under the assumption that R_J and C_J are the same for all junctions and C_g is the same for all islands, the bare and ground-capacitance models of the pump are described by just these three parameters. The particular seven-junction pump considered here has been the subject of several previous studies,[4,5,21] and its performance has been characterized in detail. We take R_J to be $\frac{1}{7}$ of the total pump resistance measured at low temperature and high voltage. For the ground-capacitance model, the ratio of C_g to C_J is determined by the relative changes in V_E observed when a single charge is transferred through each of the seven junctions. (Tunneling in junctions farther from C_E produces a smaller change in V_E due to voltage division by the intervening capacitance ladder.) Given this ratio, C_J is then chosen for both models to match the thermal broadening of single-electron transitions.

TABLE I. Circuit parameters for the bare and ground capacitance models of the seven-junction electron pump. For comparison, average values of C_J and C_g are listed for the full model, with stray capacitances included.

Model	R_J (kΩ)	C_J (aF)	C_g (aF)
Bare	470	325	0
Ground capacitance	470	220	50
Full	470	215	48

Because a single value of C_J describes the transition width over the full range of mixing-chamber temperatures T_{mc}, the electron-temperature T of the pump is assumed to equal T_{mc}. The transition widths of individual junctions also indicate that the junction capacitances are nearly uniform, differing by no more than about 10%. Based on these measurements, the parameters inferred for the bare and ground-capacitance models are listed in Table I.

The values of C_J and C_g derived for the bare and ground-capacitance models are generally larger than the physical capacitances of the junctions and gates because they are chosen as optimum fitting parameters and tend to compensate for the stray capacitances explicitly omitted from these models. A more accurate physical picture of the pump is provided by the full model, which includes stray capacitances. To determine parameters for the full model, we first estimate the stray capacitances based on the geometry of the pump.[4] The validity of such estimates is confirmed by the fact that the values of gate capacitance obtained from the geometry proved to be in good agreement with values derived from the periodicity of the pump's response to gate voltages. Thus, geometric calculations provide all of the required capacitances except the capacitance C_J' of the bare junctions. As with the other models, C_J' is chosen to fit the measured width of single-charge transitions. On this basis, the capacitance matrix $\mathbf{C}$ for the full model is[21]

$$\mathbf{C} = \begin{pmatrix} 0.0 & 218.8 & 5.8 & 2.7 & 1.7 & 1.2 & 1.0 & 0.0 \\ 218.8 & 0.0 & 213.7 & 3.3 & 1.1 & 0.6 & 0.4 & 46.7 \\ 5.8 & 213.7 & 0.0 & 213.6 & 3.3 & 1.0 & 0.6 & 46.8 \\ 2.7 & 3.3 & 213.6 & 0.0 & 213.6 & 3.3 & 1.1 & 47.2 \\ 1.7 & 1.1 & 3.3 & 213.6 & 0.0 & 213.6 & 3.3 & 48.1 \\ 1.2 & 0.6 & 1.0 & 3.3 & 213.6 & 0.0 & 213.7 & 51.3 \\ 1.0 & 0.4 & 0.6 & 1.1 & 3.3 & 213.7 & 0.0 & 264.4 \\ 0.0 & 46.7 & 46.8 & 47.2 & 48.1 & 51.3 & 264.4 & 0.0 \end{pmatrix} \text{aF}, \tag{23}$$

where C_{ij} is the capacitance between nodes i and j in Fig. 1(b). Thus, $C_{12} = 218.8$ aF is the total capacitance of the first junction, including a bare capacitance of $C_J' = 200$ aF and a stray capacitance of 18.8 aF. Similarly, $C_{28} = 46.7$ aF is the capacitance of the first gate plus the stray capacitance between the first island and ground. Having determined the

parameters of all three models, we now explore their predictions for the leakage current without further adjustments.

D. Experiment

Because stray charge in the dielectric materials of the pump usually creates an unknown offset that adds to the
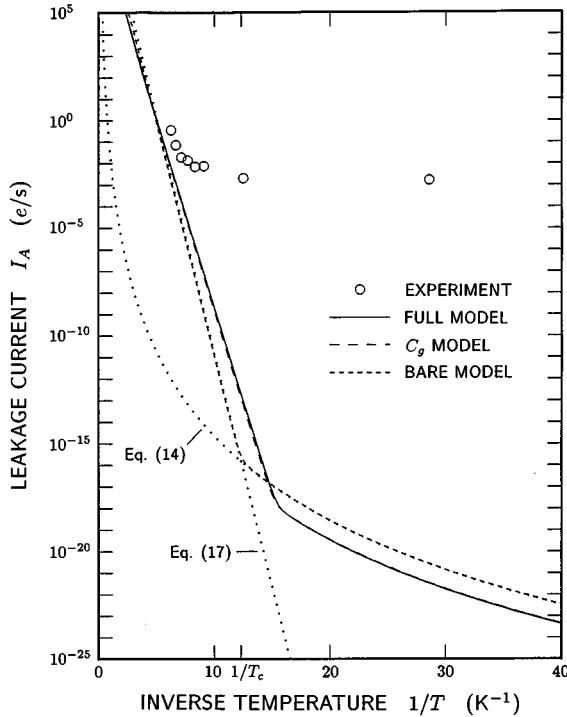
FIG. 5. Absolute leakage current as a function of inverse temperature for a seven-junction electron pump in the absence of voltage or charge biases, $V_E = Q_i = 0$. Circles show experimental results, while I_A is plotted for the full, ground-capacitance, and bare models with a solid line, long dashes, and short dashes, respectively. Dotted lines plot asymptotic formulas, Eqs. (14) and (17), applicable to the bare model. The inverse crossover temperature is also indicated for the bare model.

applied gate voltages, leakage currents have often been measured for pumps or junction arrays in which the bias state is uncontrolled. In the experiments reported here, care was taken to determine offsets and accurately control the bias state of the pump. The problem of accurate control is complicated by the existence of stray capacitances, which couple some fraction of the voltage applied to a given gate lead to all islands of the pump. As detailed elsewhere,[3,4] such cross coupling can be electronically cancelled using a matrix of amplifiers adjusted to apply suitable correction voltages to the cross-coupled gates. When cross coupling is cancelled in this way, a charge bias can be applied to one and only one island, as idealized in the ground-capacitance model. To compensate for gate bias offsets due to stray charge, the zero-bias setpoints are adjusted to minimize the error rate in the pumping mode. Spot checks, based on the observed thresholds for single-charge transitions,[5] reveal that adjustment for minimum pumping error yields zero-bias setpoints within 0.1 e of the actual zero charge bias. Finally, because the charge on C_E adjusts itself until the rates of forward and reverse leakage are equal, leakage experiments are naturally performed near zero voltage. Thus, the bias state of the pump during our leakage measurements is well described by $V_E = Q_i = 0$.

Experimental and theoretical results for the absolute leakage current of a seven-junction pump are plotted as a function of inverse temperature in Fig. 5 to create an Arrhenius

plot. Experimental values of I_A are derived from records of the charge on C_E, like that shown in Fig. 2, simply by counting the number of single-charge jumps observed over an interval of time. As Fig. 5 shows, the experimental I_A is thermally activated at temperatures above about 140 mK and approaches a plateau at lower temperatures.

Figure 5 also shows values of leakage current computed for the bare, ground-capacitance, and full models of the electron pump. The utility of the C_g model is apparent here in that the predicted I_A is virtually indistinguishable from that of the full model. While the bare model is in rough agreement with the full model, there are significant quantitative differences. This discrepancy is to be expected, however, given that the bare model does not explicitly account for the gate capacitance. On the other hand, the asymptotic formulas for I_A, Eqs. (14) and (17), are in excellent agreement with the bare model from which they derive. This agreement confirms that leakage is dominated by Nth-order cotunneling below the crossover temperature and by first-order (single-junction) processes above T_c. Contributions by processes of intermediate order are apparently not important at any temperature.

In the thermally activated region above 140 mK, experiment and theory are in good agreement. Here, the experimental leakage is about two orders of magnitude larger than the theoretical I_A, but the activation energy (slope of the Arrhenius plot) agrees within the accuracy of the experiment. Given that this comparison involves no adjustment of parameters, we take the agreement as confirmation of the theory in the high-temperature regime. As the temperature of the mixing chamber is lowered below 140 mK, however, direct measurements confirm that the electron temperature of the pump continues to equal T_{mc},[5] but the leakage current fails to follow the theoretical prediction. At 35 mK the experimental leakage is almost nineteen orders of magnitude greater than theory. As noted previously, this discrepancy clearly indicates that the theory presented here omits an important source of leakage that dominates at low temperatures. While the excess leakage might be due to environmental noise, as suggested by Martinis and Nahum,[19] the case for this mechanism is not proven, and the cause remains open to speculation.

Although the leakage rate observed at low temperatures is orders of magnitude higher than predicted by theory, the rate at 35 mK corresponds to leakage of just one charge in 10 min on average. Fortunately, this rate is low enough to allow capacitance calibrations of high accuracy. Thus, while our understanding of leakage mechanisms is incomplete, leakage does not present a practical barrier to metrological application of the pump.

To further explore leakage in the electron pump, we have measured I_A as a function of a charge bias Q_{J4} applied to the central junction. By definition, a charge bias Q_{Ji} is obtained on junction i by applying a gate bias $Q_{i-1} = Q_{Ji}$ to the island on the junction's left and a gate bias $Q_i = -Q_{Ji}$ to the island on its right. When $Q_{Ji} = 0$, the Coulomb blockade is maximally effective in preventing tunneling through junction i, and we expect to observe a minimum in the leakage rate. However, when $Q_{Ji} = \pm e/2$, the Coulomb blockade is effectively eliminated, and the leakage rate is expected to be maximum.
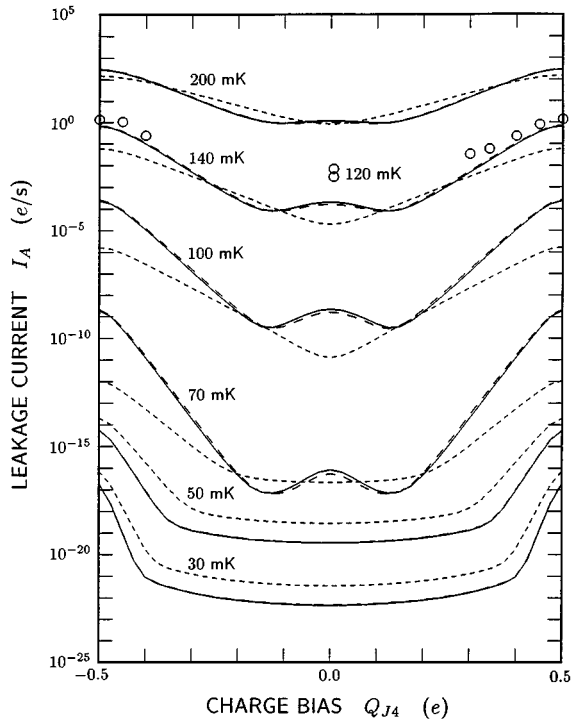
FIG. 6. Absolute leakage current I_A as a function of a charge bias Q_{J4} applied to the central junction of a seven-junction electron pump. In this case the applied biases are $V_E = Q_1 = Q_2 = Q_5 = Q_6 = 0$, $Q_3 = Q_{J4}$, and $Q_4 = -Q_{J4}$. Circles show experimental results for $T = 120$ mK, while solid lines, long dashes, and short dashes plot I_A for the full, ground-capacitance, and bare models, respectively, at a variety of temperatures. The two experimental points at $Q_{J4} = 0$ were taken at the beginning and end of data acquisition to verify that charge offsets had not changed in the interim.

These expectations are met in part by the data shown in Fig. 6. Here, we plot I_A as a function of Q_{J4} for an experiment performed at 120 mK and for the three theoretical models evaluated at a variety of temperatures. As anticipated, I_A is always greater at $Q_{J4} = \pm e/2$ than at $Q_{J4} = 0$. Indeed, the experimental points can be connected by a smooth curve with a minimum at $Q_{J4} = 0$ and maxima at $Q_{J4} = \pm e/2$. Thus, we were surprised to discover that the full and C_g models predict minima near $Q_{J4} = \pm 0.13\, e$. While our limited experimental data are consistent with this prediction, confirmation would require additional experiments. However, overall agreement between theory and experiment is good, given that the experiment was performed at a temperature somewhat below that for which the theory is thought to apply.

Why do the full and C_g models predict minima in the leakage current near $Q_{J4} = \pm 0.13\, e$? To answer this question, we look more closely at leakage processes in the relevant temperature range, $T_c \ll T \ll E_C / k_B$, where through transfers are dominated by thermally activated, single-junction (first-order) tunneling. Since tunneling can occur in either direction and in any order among the N junctions, there are a total of $2N!$ through processes involving only first-order tunneling. According to Eqs. (14) and (16), each such process contributes to I_A in proportion to an Arrhenius factor $\exp(-E_A/k_B T)$, where E_A is an activation energy given by
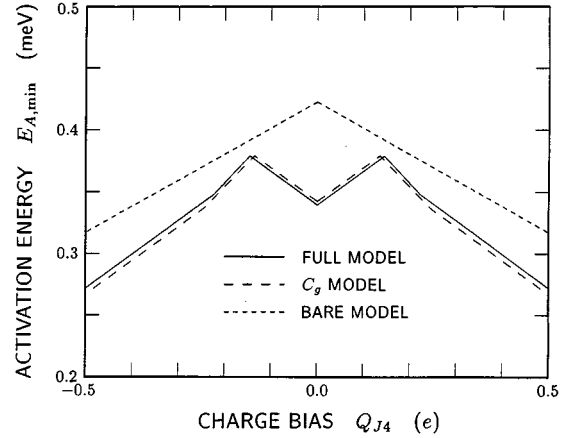
FIG. 7. Minimum activation energy $E_{A,\min}$ for leakage processes in the intermediate temperature regime ($T_c \ll T \ll E_C / k_B$) as a function of charge bias Q_{J4} on the central junction of a seven-junction electron pump. Calculated results are shown for the full, gate-capacitance, and bare models using solid lines, long dashes, and short dashes, respectively. The applied biases are $V_E = Q_1 = Q_2 = Q_5 = Q_6 = 0$, $Q_3 = Q_{J4}$, and $Q_4 = -Q_{J4}$.

$$E_A = \sum_{i=1}^{N} \delta E_i \theta(\delta E_i). \qquad (24)$$

Here, θ is the unit step function, and only tunneling steps with positive δE add to E_A. Because E_A is generally much larger than $k_B T$, the leakage rate is very sensitive to the activation energy, making the dominant processes those with the smallest E_A. Thus, we expect I_A to scale roughly as $\exp(-E_{A,\min}/k_B T)$, where $E_{A,\min}$ is the minimum activation energy over all processes. This minimum energy is plotted as a function of Q_{J4} in Fig. 7 for all three models of the pump. As expected, $E_{A,\min}$ shows a single maximum at $Q_{J4} = 0$ for the bare model but symmetric maxima at $Q_{J4} \approx \pm 0.13\, e$ for the full and C_g models. Thus, the minima in I_A directly reflect maxima in the minimum Coulomb barrier energy for each model.

To understand the differences between these models more completely, we examine the dominant leakage processes in greater detail. For the bare model at $Q_{J4} = 0$, the δE_i are the same for all $2N! = 10\,080$ processes, so that each process has the same E_A and contributes identically to I_A. This symmetry is broken for $|Q_{J4}| > 0$, and at $|Q_{J4}| = 0.1\, e$ the minimum E_A is attained by only 4 320 processes, while at $|Q_{J4}| = 0.5\, e$ the processes with minimum E_A are reduced to 1 440. As might be anticipated, the dominant processes at $|Q_{J4}| = 0.5\, e$ are those in which tunneling first occurs in the central junction, creating a dipole that offsets the applied charge bias. In the bare model, such dipole processes are energetically favorable at all charge biases. In the full and C_g models, on the other hand, the minimum E_A at $Q_{J4} = 0$ is represented by only 16 processes, and these do not include dipole processes. In these models, the activation energies for the processes dominant at $Q_{J4} = 0$ increase with increasing $|Q_{J4}|$ while those for dipole processes decrease, such that some dipole processes become dominant for $|Q_{J4}| > 0.13\, e$. Thus, the minima in leakage at $Q_{J4} \approx \pm 0.13\, e$ result from a
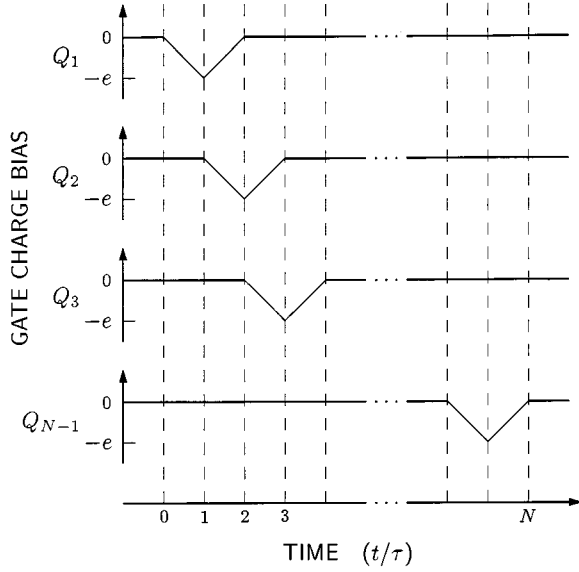
FIG. 8. Charge biases applied to the $N-1$ gates of an N-junction pump to transfer a charge e through the pump.

FIG. 9. Charge Q_E on external capacitor C_E as a function of time for a seven-junction pump being used to shuttle a single charge back and forth once every 350 ns. The ramp time τ of the applied charge bias is 25 ns and the temperature is 33 mK.

competition between different processes that is absent from the bare model due to its greater symmetry.

Having explored the bare, ground-capacitance, and full models in some detail, we conclude that the bare model is useful as a basis for asymptotic formulas and rough estimates of basic pump operation. However, the bare model fails to account even qualitatively for some effects predicted by the more complete models. Also, at least for the case presented here, the ground-capacitance model is in excellent quantitative agreement with the full model, in spite of its simplified capacitance matrix.

III. COUNTING ERRORS

Although leakage in the hold mode is an important consideration for capacitance standards, the fundamental utility of an electron pump is determined by counting errors. In principle, a pump transfers a single charge between input and output in response to a sequence of gate charge biases like those shown in Fig. 8. Here, each gate in succession receives a triangular pulse of duration 2τ and amplitude $-e$, which usually moves one charge from the input through the successive islands to the output. However, this process occasionally fails to transfer a charge or transfers an extra charge, resulting in a counting error.

To measure counting errors experimentally, the pump is used to shuttle a single charge back and forth between input and output while the charge Q_E on the external capacitor C_E is monitored using an electrometer. In this experiment, gate pulses are applied alternately as shown in Fig. 8 (to move a charge from input to output) and in reverse order (to move a charge from output to input). Because charge shuttling is typically driven at a few megahertz, much faster than the response time of the electrometer, the measured Q_E appears to be constant except when the pump makes an error. Thus, experimental traces of Q_E, like that shown in Fig. 9, do not record the rapid changes in charge associated with shuttling but do reveal when the pump fails to transfer a charge, in this
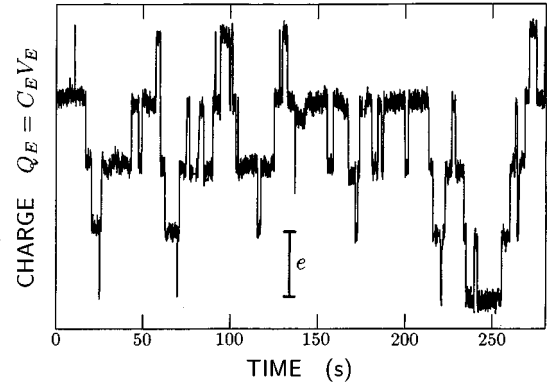
instance about once every 3 seconds on average. While this error rate may seem high, it corresponds to a shuttle error of about $\mathcal{E}_S = 5 \times 10^{-8}$ or 50 errors in 10^9 pump cycles. Thus, the shuttle test provides a sensitive measure of infrequent errors.

A. Simulation

Calculation of the charge error $\mathcal{E}_Q = ||Q|/e - 1|$ is based on accurate evaluation of the charge Q transferred by the pump during a single bias cycle. In the procedure adopted here, Eq. (1) is integrated using a fourth-order Runge–Kutta algorithm to determine the probabilities P_n for occupation of the charge states n as a function of time, and Q is evaluated by integrating the current given by Eq. (2). Although the charge on each island is restricted to the values of 0 and $\pm e$, this yields a total of $3^6 = 729$ possible charge states for a seven-junction pump. To reduce the calculation to a manageable size, charge states are included only during the portion of the bias cycle when they are active. During integration, a charge state is added when the rate of transition to the state exceeds a specified bound and a charge state is removed when its probability drops below another bound. Both bounds are chosen to be small enough that they do not affect the results. Integration is continued for a brief period after the bias cycle is complete to assure that Q is fully converged. Finally, because $\mathcal{E}_Q$ is determined by a small difference between two numbers close to 1, calculations are performed using 33 digit arithmetic. This extended precision allows accurate evaluation of $\mathcal{E}_Q$ for errors as small as about 10^{-25}.

Because the errors in a shuttle experiment are of both signs, we might anticipate that evaluation of the shuttle error $\mathcal{E}_S = (Q_+ + Q_-)/e$ requires that positive and negative errors be tabulated separately, as for the absolute leakage current I_A. However, $\mathcal{E}_S$ can usually be computed from the net charge errors computed for forward and reverse pumping, $\mathcal{E}_Q^+$ and $\mathcal{E}_Q^-$. The reason can be understood from Fig. 10, which plots $\mathcal{E}_Q^+$ and $\mathcal{E}_Q^-$ as a function of bias voltage. As Fig. 10 shows, $\mathcal{E}_Q^+$ goes to zero at a voltage near $V_E = 46$ μV, where positive and negative errors exactly cancel. For voltages somewhat less than 46 μV virtually all of the errors in forward pumping result from a failure to transfer a charge,
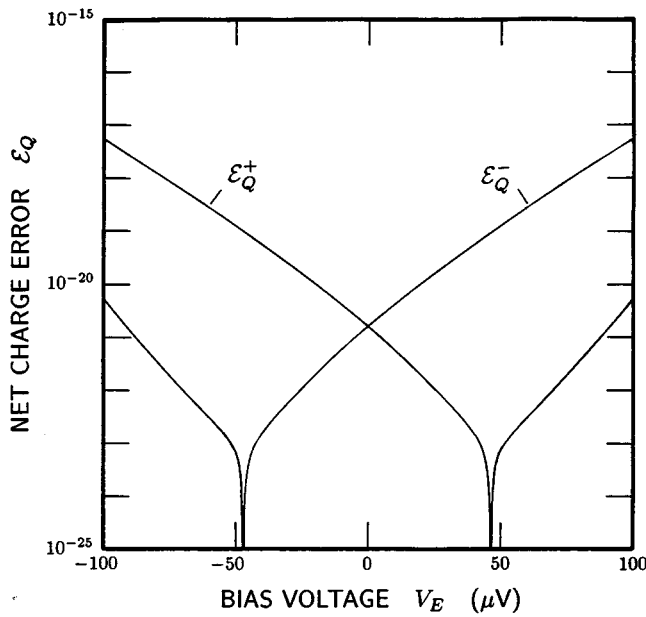
FIG. 10. Net charge error for forward and reverse pumping, $\mathcal{E}_Q^+$ and $\mathcal{E}_Q^-$, as a function of bias voltage V_E calculated for the ground-capacitance model of a seven-junction electron pump. The system parameters are $R_J = 470$ kΩ, $C_J = 220$ aF, $C_g = 50$ aF, $\tau = 40$ ns, and $T = 25$ mK.

FIG. 11. Electrostatic energy E as a function of the location of an extra charge on the six islands of a seven-junction pump (solid lines), calculated within the bare model for $V_E = 0$. Plots are shown for the beginning and end of the pump cycle ($t = 0$ and 7τ) and at times $t = j\tau$ ($j = 1, \ldots, 6$) when the gate charge bias on island j is at its peak. Dashed lines show the energy when a second extra charge is introduced on successive islands of the pump, with the first extra charge held on the island of minimum energy, as indicated by a filled circle. As the figure illustrates, the pump allows a charge to move from island to island as successive gate charge pulses are applied, but a second charge is prevented from entering the pump by the Coulomb blockade. Island number 0 refers to the input and output electrodes.

while for voltages somewhat greater than 46 μV the errors result from transfer of an extra charge. That is, except at voltages within a few microvolts of $V_E = 46$ μV, $\mathcal{E}_Q^+$ represents either almost purely positive or purely negative errors. Given that $\mathcal{E}_S$ is an average over forward and reverse pumping cycles, we can write $\mathcal{E}_S \approx (\mathcal{E}_Q^+ + \mathcal{E}_Q^-)/2$, since $\mathcal{E}_Q^+$ and $\mathcal{E}_Q^-$ each contribute significantly to this sum only at voltages where they represent errors of predominantly one sign. This approximation is valid as long as the voltages at which $\mathcal{E}_Q^+ = 0$ and $\mathcal{E}_Q^- = 0$ are not too close to $V_E = 0$.

In experimental measurements of the shuttle error, the charge Q_E on the external capacitor adjusts itself until the rates of positive and negative errors are equal. This balance is illustrated by the data presented in Fig. 9 and results in a bias voltage near $V_E = 0$ (cf. Fig. 10). Thus, our shuttle error data was taken near zero voltage bias using applied gate charge biases like those plotted in Fig. 8, and we focus on this case in the remainder of the paper.

B. Asymptotic formulas

As with leakage errors, asymptotic formulas can be derived for counting errors within the bare model of the electron pump. We consider three types of error investigated previously by Jensen and Martinis:[8] errors due to failure to tunnel in the limit of short pulse widths, errors due to thermally activated, single-junction tunneling at intermediate temperatures, and errors due to cotunneling in the limit of low temperature. The resulting asymptotic formulas provide a useful check on our simulations and help identify the error mechanisms active in each regime.

Insight into the operation of the pump is provided by examining the pump's electrostatic energy for various charge

and bias states. In Fig. 11, solid lines plot the energy when a single extra charge is introduced on each island of the pump in succession. Plots are shown for the bare model at the beginning and end of the pump cycle ($t = 0$ and 7τ) and at times $t = j\tau$ ($j = 1, \ldots, 6$), when the gate charge bias on island j is at its peak. At $t = 0$, when there is no applied bias, introducing a charge on any island raises the pump's energy, and charge transfer is blocked. At $t = \tau$, when the charge bias on island 1 is $-e$, the pump's energy is lowered if an extra charge tunnels onto this island. As time advances to $t = 2\tau, \ldots, 7\tau$, a charge bias is applied to each island in succession, the energy minimum moves from island to island, and the extra charge is expected to tunnel through successive junctions until it reaches the output electrode. Dashed lines in Fig. 11 show the energy when a second extra charge is introduced on successive islands of the pump, with the first extra charge held on the island of minimum energy, as indicated by the filled circle. In each case, the second extra charge encounters an energy barrier that blocks it from tunneling onto an island. Thus, the pump is expected to transfer

one and only one electron during each bias cycle. However, while this expectation is nearly always met, occasional errors do occur.

1. Failure-to-tunnel errors

In examining counting errors, we consider first the case in which the charge bias pulses are so short that tunneling fails to occur while it is energetically favorable. This case was considered by Jensen and Martinis,[8] who derive an approximate error probability under the assumption that an error will result if tunneling onto an island does not happen before the charge bias on the island reaches its maximum. They note, however, that this assumption is unnecessarily restrictive, since tunneling remains energetically favorable long after the charge bias peaks. For example, tunneling between islands 1 and 2 is energetically favorable ($\delta E < 0$) over the interval $1.5 < t/\tau < 5$, as shown in Fig. 11, rather than just for $1.5 < t/\tau < 2$. Thus, we can extend the arguments of Jensen and Martinis to derive a more accurate estimate of failure-to-tunnel errors by considering the entire window of opportunity for tunneling.

We restrict our attention to the seven-junction pump in the limit of zero temperature. In this limit, failure to tunnel is most probable in junctions 2, 3, and 4, and the probability P of failure is the same for each of these junctions. Since the probability of tunneling through all three junctions is $(1-P)^3$, the shuttle error is given by

$$\mathcal{E}_S = 1 - (1-P)^3, \quad (\tau \ll \tau_c, \ V_E = 0, \ T = 0, \ N = 7) \tag{25}$$

which is expected to be valid for τ less than some temperature-dependent crossover halfwidth τ_c, beyond which other error processes dominate. The probability P can be evaluated without further approximation using the expressions for δE given by Jensen and Martinis. Taking into account the fact that the charge can tunnel backward as well as forward during the last τ of its window of opportunity (for example, a charge on island 1 can tunnel back to the input electrode as well as ahead to island 2 during the interval $4 < t/\tau < 5$, as shown in Fig. 11), we obtain

$$P = (7R_J C_J/\tau)[1 - \exp(-\tau/7R_J C_J)]\exp(-19\tau/28R_J C_J). \tag{26}$$

In this expression, the final exponential factor accounts for failure to tunnel during the first 2.5τ of the window of opportunity and the two prefactors account for the final τ. Noting that $\mathcal{E}_S \approx 3P$ for $P \ll 1$, we find that failure-to-tunnel errors decrease exponentially with increasing pulse width, as expected from previous work.[8]

2. Thermal errors

The dominant thermal errors occur late in the bias cycle, after the possibility of forward tunneling through junction 1 has been blocked. In particular, for the situation at $t = 5\tau$ in Fig. 11, an error can result if thermal energy is available to move the charge from island 5 back to the input electrode. Although this is an improbable process, it is likely to produce an error if it happens, because forward tunneling through junction 1 is also improbable. As might be expected, the pump is most susceptible to thermal errors when the
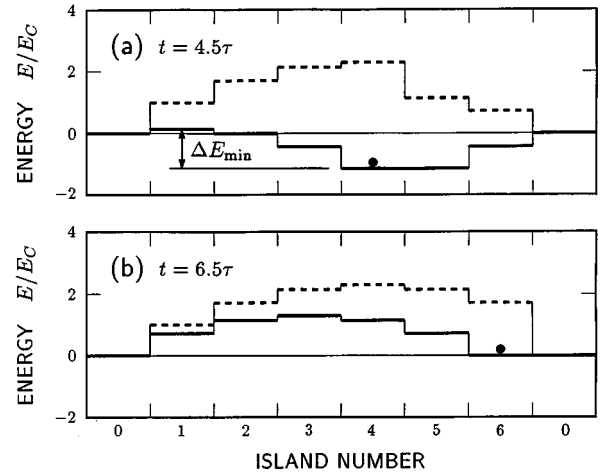
FIG. 12. Electrostatic energy E as a function of the location of an extra charge on the six islands of a seven-junction pump (solid lines), calculated within the bare model for $V_E = 0$. Plots are shown for the bias conditions at (a) $t = 4.5\tau$, when thermal errors are maximum, and at (b) $t = 6.5\tau$, when cotunneling errors of order $n - 1$ first become possible at $T = 0$. Dashed lines show the energy when a second extra charge is introduced on successive islands of the pump, with the first extra charge held on the indicated island.

energy barrier for returning to the input electrode is minimum. In the seven-junction pump, this minimum occurs at $t = 4.5\tau$, as shown in Fig. 12(a). The minimum energy barrier is identified here as $\Delta E_{\min}$. A detailed analysis of this case by Jensen and Martinis yields for the shuttle error,[8]

$$\mathcal{E}_S = \frac{N!}{8[(N-1)/2]![(N+1)/2]!} \frac{\tau k_B T}{R_J C_J E_C}$$
$$\times \exp(-\Delta E_{\min}/k_B T),$$

$$(C_g = 0, \ \tau \gg \tau_c, \ V_E = 0, \ T_c' \ll T \ll E_C/k_B, \ N \ \text{odd}), \tag{27}$$

where

$$\Delta E_{\min} = E_C(N-1)^2/4N, \quad (N \ \text{odd}). \tag{28}$$

This result is expected to be valid at intermediate temperatures $T_c' \ll T \ll E_C/k_B$, where T_c' is a crossover temperature, below which cotunneling processes dominate. As Eq. (27) indicates, errors at intermediate temperatures are governed by an Arrhenius factor with an activation energy of $\Delta E_{\min}$.

3. Cotunneling errors

In the limit of low temperature, $T \ll T_c'$, thermal processes are frozen out, and cotunneling errors dominate. Although leakage involving Nth-order cotunneling can occur throughout the bias cycle, there is a brief interval during which cotunneling of order $N - 1$ is possible, and these lower-order processes yield more counting errors. If we consider the $T = 0$ limit, then cotunneling can occur only when the net change in electrostatic energy is negative. Because the extra charge proceeding through the pump is usually on an island at lower energy than the input or output electrode (cf. Fig. 11), it generally cannot escape by cotunneling. However,

near the end of the bias cycle, at $t=6.5\tau$, the energy of the extra charge on island 6 is equal to the energy it would have on either the input or output electrode. This equal-energy condition is illustrated in Fig. 12(b). As t increases beyond 6.5τ, the energy of island 6 rises above that of the input and output electrodes, and the charge can leave the pump either by first-order tunneling to the output electrode or by cotunneling of order $N-1$ to the input electrode. Although the latter process is unlikely compared to the former, it is the dominant error process at low temperatures.

Jensen and Martinis have analyzed cotunneling errors for the general case of finite voltages.[8] However, by considering the special case of $V_E=0$, we obtain a simplified derivation requiring fewer approximations. To sketch this calculation, let $t'=t-(N-1/2)\tau$, let $P(t')$ be the probability that the extra charge is on island $N-1$, and let $\Gamma_o(t')$ and $\Gamma_i(t')$ be the rates of tunneling from island $N-1$ to the output and input electrodes. In the limit of zero temperature, the cotunneling error is then given by

$$\mathcal{E}_S = \int_0^\infty P(t')\Gamma_i(t')dt', \qquad (29)$$

where P satisfies the approximate equation

$$dP/dt' = -\Gamma_o P, \quad P(0)=1, \qquad (30)$$

in the limit $\Gamma_o \gg \Gamma_i$. From Jensen and Martinis we have

$$\Gamma_o = \frac{(N-1)t'}{NR_JC_J\tau}, \quad (0 \leqslant t' \leqslant \tau/2) \qquad (31)$$

$$\Gamma_i = \frac{K}{R_KC_J}\left(\frac{R_K}{R_J}\right)^{N-1}\left(\frac{t'}{\tau}\right)^{2N-3}, \quad (0 \leqslant t' \leqslant \tau/2) \qquad (32)$$

where

$$K = \frac{(N-1)^{2N-1}}{\pi^{2N-4}N(2N-3)![(N-2)!]^2}. \qquad (33)$$

For these rates we find

$$P = \exp\left[-\frac{(N-1)t'^2}{2NR_JC_J\tau}\right], \quad (0 \leqslant t' \leqslant \tau/2) \qquad (34)$$

and

$$\mathcal{E}_S = \frac{(2N)^{N-2}(N-1)^N}{\pi^{2N-4}(N-2)!(2N-3)!}\left(\frac{R_KC_J}{\tau}\right)^{N-2},$$

$$(C_g=0, \quad \tau \gg \tau_c, \quad V_E=0, \quad T=0) \qquad (35)$$

where the integrand in Eq. (29) was evaluated using Eqs. (32) and (34) even for $t'>\tau/2$, since the contribution from large times is insignificant. The functional dependence of $\mathcal{E}_S$ on R_K, C_J, and τ given by Eq. (35) agrees with the result of Jensen and Martinis, but the prefactor differs by a factor of about 60 for $N=7$. In any case, cotunneling errors fall off with increasing pulse width as $1/\tau^{N-2}$, reflecting the fact Γ_o/Γ_i is larger for smaller t' and tunneling to the output is more nearly certain if the pump passes slowly through the equal-energy condition illustrated in Fig. 12(b).
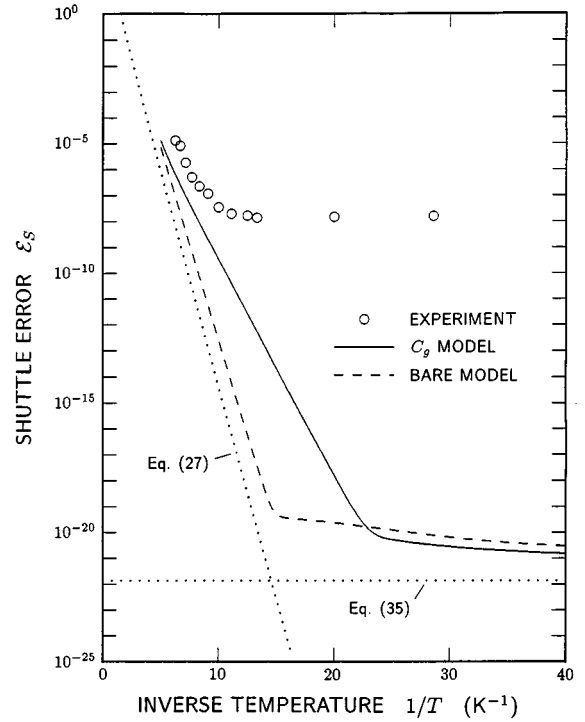
FIG. 13. Shuttle error $\mathcal{E}_S$ as a function of inverse temperature for a seven-junction electron pump with the halfwidth of the gate bias pulse fixed at $\tau=40$ ns. Circles show experimental results, while calculations for the ground-capacitance and bare models are plotted as solid and dashed lines. Parameters for the C_g model are $V_E=0$, $R_J=470$ kΩ, $C_J=220$ aF, and $C_g=50$ aF, while for the bare model $C_J=325$ aF and $C_g=0$. Dotted lines show asymptotic formulas for the bare model.

C. Experiment

Having developed simulations and asymptotic formulas for the shuttle error, we are ready to compare these predictions with experimental measurements. In this section, we examine shuttle error as a function of both temperature and the width of the gate bias pulse.

Figure 13 displays results for $\mathcal{E}_S$ as a function of inverse temperature for the seven-junction pump driven with bias pulses of 40 ns halfwidth. This figure compares experimental results with simulations for the C_g and bare models and with two asymptotic formulas. The parameters used in the simulations and formulas are identical to those discussed previously, and no adjustments were made to improve the fit with experiment. At temperatures above about 100 mK, the experimental data reveal an exponential behavior characteristic of thermal activation, and there is good agreement with simulations for the C_g model. In particular, the activation energy (slope of the Arrhenius plot) agrees with that of the C_g model within experimental error, and the magnitude of $\mathcal{E}_S$ exceeds the predictions of the model by only about an order of magnitude.

At temperatures less than 100 mK, however, there are substantial differences between experiment and simulation. Below 100 mK, the experiment shows a plateau in $\mathcal{E}_S$ near 10^{-8}, while the C_g model predicts that $\mathcal{E}_S$ will plateau only when the temperature drops below 45 mK, where it reaches 10^{-20}. Because independent experiments confirm that the

electron temperature of the pump follows the temperature of the mixing chamber, we conclude that the shuttle errors at low temperatures, like leakage errors, are dominated by a mechanism not included in the orthodox theory of the pump. All the same, the experimentally observed shuttle error of 1.5×10^{-8} is small enough to allow construction of a capacitance standard with an accuracy competitive with the best available standards.

As might be expected, calculations of $\mathcal{E}_S$ based on simulation of the bare model agree less well with experiment than those for the C_g model. Results for the bare model are included here primarily to validate the analytic formulas derived from it. While agreement is not perfect, Fig. 13 shows that Eqs. (27) and (35) give good estimates of the simulated $\mathcal{E}_S$ for temperatures in the ranges $T \gg T_c$ and $T \ll T_c$, respectively, where the crossover temperature is roughly $T_c = 60$ mK. We conclude that, within the bare model, shuttle errors at intermediate temperatures occur primarily by thermally activated tunneling back to the input electrode and at low temperatures by cotunneling of order $N-1$. Since the experimental $\mathcal{E}_S$ is thermally activated above 100 mK, the error mechanism is probably the same as that identified for the bare model, and the slope of the experimental Arrhenius plot, about 0.2 meV, can be interpreted as the minimum energy $\Delta E_{\min}$ required for the charge to return to the input electrode. Thus, shuttle errors at intermediate temperatures appear to be well understood.

Figure 14 shows the shuttle error at 33 mK as a function of bias-pulse halfwidth for the seven-junction pump. Again, we compare experiment with simulations for the C_g and bare models and with two asymptotic formulas. Because the data are for a relatively low temperature, we do not expect the experimental shuttle error to be governed by mechanisms described by the orthodox theory, and the data shown in Fig. 14 confirm this expectation. Thus, the experimental $\mathcal{E}_S$ exceeds the prediction of the ground-capacitance model by 14 orders of magnitude in the limit of long pulses. According to experiment, the shuttle error decreases exponentially with increasing pulse width for values of τ up to about 30 ns, above which $\mathcal{E}_S$ plateaus at an error of about 1.5×10^{-8}. While this behavior is superficially similar to theoretical predictions, the quantitative discrepancies are so large that the experimentally observed errors almost certainly involve an effect not included in the theory.

Comparing the bare-model simulation with the associated asymptotic formulas plotted in Fig. 14, we conclude that Eqs. (25) and (35) reproduce the τ dependence of the bare model with reasonable accuracy. Thus, the exponential form observed for τ less than about 10 ns can be associated with failure-to-tunnel errors. In this regime, we can define a characteristic time t_1 such that $\mathcal{E}_S \propto \exp(-\tau/t_1)$. According to Eqs. (25) and (26), this time is $t_1 = 4R_J C_J/3 = 0.20$ ns, while the slope of the ground-capacitance curve in Fig. 14 yields $t_1 = 0.37$ ns. By comparison, the slope of the experimental curve for $6 < \tau < 30$ ns corresponds to $t_1 = 4.3$ ns. Again, the discrepancy between theory and experiment suggests that the actual error mechanism differs substantially from that of the orthodox theory.

What mechanisms beyond the orthodox theory might explain the experimentally observed shuttle errors? While previous experiments on this particular device have ruled out
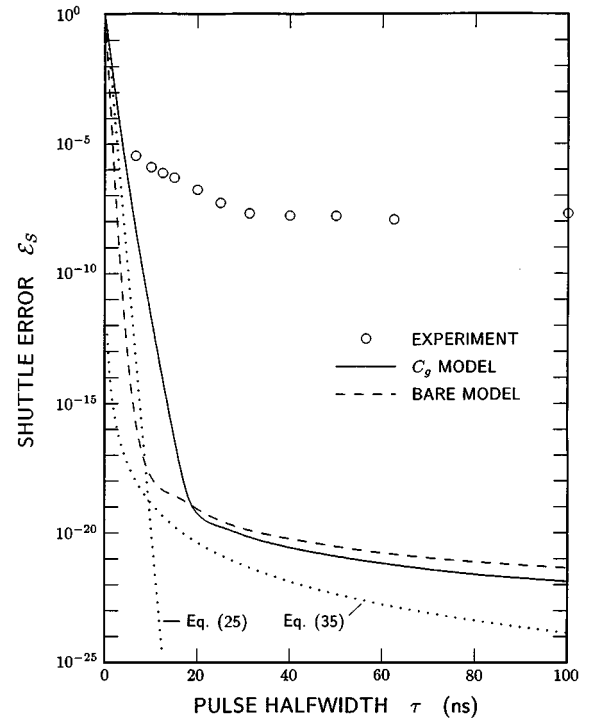
FIG. 14. Shuttle error $\mathcal{E}_S$ at 33 mK as a function of the halfwidth of the gate bias pulse used to drive a seven-junction electron pump. Circles show experimental results, while calculations for the ground-capacitance and bare models are plotted by solid and dashed lines. Parameters for the C_g model are $V_E = 0$, $R_J = 470$ kΩ, $C_J = 220$ aF, and $C_g = 50$ aF, while for the bare model $C_J = 325$ aF and $C_g = 0$. Dotted lines show asymptotic formulas for the bare model.

the possibility that cosmic rays contribute significantly to the error rate,[4,5] the explanation may involve photon-assisted tunneling produced both by environmental noise and the cyclic bias. In particular, the exponential decrease in $\mathcal{E}_S$ observed for $6 < \tau < 30$ ns is consistent with the strong frequency dependence expected for errors due to photon-assisted tunneling driven by the cyclic bias,[20] while the plateau in $\mathcal{E}_S$ observed for $\tau > 30$ ns is consistent with photon-assisted tunneling driven by environmental noise.[19] Clearly, both of these mechanisms warrant further investigation.

IV. CONCLUSION

By comparing experimentally measured leakage and counting errors with the results of orthodox theory, including cotunneling, for three different models of the electron pump, we have established the accuracy of the theory at intermediate temperatures and shown that the orthodox theory is inadequate to explain errors observed at low temperatures. In the intermediate temperature regime, both leakage and counting errors are due to thermally activated, single-junction processes that move the pump over an energy barrier. Counting errors in this regime result during the latter part of the bias cycle, when tunneling from the input electrode to the first island is nominally blocked and the extra electron is occasionally returned to the input by thermal activation.

Comparison of leakage errors predicted by the bare, ground-capacitance, and full models, indicates that the full and ground-capacitance models are virtually indistinguishable for the cases considered, while the bare model generally gives good approximate results. However, the bare model fails to predict a double minimum in the leakage as a function of charge bias on the central junction.

The failure of the orthodox theory to explain the errors observed at low temperatures is a result of primary impor-tance. If counting errors were as infrequent as predicted, the accuracy of the seven-junction pump would far exceed that required for fundamental metrology. The excess errors observed experimentally, while low enough to allow fabrication of a useful capacitance standard, require an explanation if further improvements are to be made. Indeed, full exploitation of the electron pump presently awaits verification that the limiting errors are due to photon-assisted tunneling[19,20] or some other cause.

[1] H. Pothier, P. Lafarge, P. F. Orfila, C. Urbina, D. Esteve, and M. H. Devoret, Physica B **169**, 573 (1991); C. Urbina, H. Pothier, P. F. Lafarge, P. F. Orfila, D. Esteve, and M. Devoret, IEEE Trans. Magn. **27**, 2578 (1991); H. Pothier, P. Lafarge, C. Urbina, D. Esteve, and M. H. Devoret, Europhys. Lett. **17**, 249 (1992).

[2] E. R. Williams, R. N. Ghosh, and J. M. Martinis, J. Res. Natl. Inst. Stand. Technol. **97**, 299 (1992).

[3] J. M. Martinis, M. Nahum, and H. D. Jensen, Phys. Rev. Lett. **72**, 904 (1994); Physica B **194-196**, 1045 (1994).

[4] M. W. Keller, J. M. Martinis, N. M. Zimmerman, and A. H. Steinbach, Appl. Phys. Lett. **69**, 1804 (1996); M. W. Keller, J. M. Martinis, A. H. Steinbach, and N. M. Zimmerman, IEEE Trans Instrum. Meas. **46**, 307 (1997).

[5] M. W. Keller, J. M. Martinis, and R. L. Kautz, Phys. Rev. Lett. **80**, 4530 (1998).

[6] D. V. Averin and K. K. Likharev, in *Mesoscopic Phenomena in Solids,* edited by B. L. Altschuler, P. A. Lee, and R. A. Webb (Elsevier, Amsterdam, 1991), p. 173.

[7] H. Pothier, Ph.D. thesis, University of Paris 6, 1991.

[8] H. D. Jensen and J. M. Martinis, Phys. Rev. B **46**, 13 407 (1992).

[9] D. V. Averin, A. A. Odintsov, and S. V. Vyshenskii, J. Appl. Phys. **73**, 1297 (1993).

[10] R. W. Rendell, Phys. Rev. B **52**, 4684 (1995).

[11] L. R. C. Fonseca, A. N. Korotkov, and K. K. Likharev, J. Appl. Phys. **79**, 9155 (1996).

[12] L. R. C. Fonseca, A. N. Korotkov, and K. K. Likharev, Appl. Phys. Lett. **69**, 1858 (1996).

[13] T. A. Fulton, P. L. Gammel, and L. N. Dunkleberger, Phys. Rev. Lett. **67**, 3148 (1991).

[14] P. D. Dresselhaus, L. Ji, S. Han, J. E. Lukens, and K. K. Likharev, Phys. Rev. Lett. **72**, 3226 (1994).

[15] P. Lafarge, P. Joyez, H. Pothier, A. Cleland, T. Holst, D. Esteve, and M. H. Devoret, C. R. Acad. Sci. Paris **314**, 883 (1992).

[16] D. V. Averin and A. A. Odintsov, Phys. Lett. A **140**, 251 (1989); Zh. Éksp. Teor. Fiz. **96**, 1349 (1989) [Sov. Phys. JETP **69**, 766 (1989)].

[17] L. R. C. Fonseca, A. N. Korotkov, K. K. Likharev, and A. A. Odintsov, J. Appl. Phys. **78**, 3238 (1995).

[18] M. B. A. Jalil, M. Wagner, and H. Ahmed, J. Appl. Phys. **85**, 1203 (1999).

[19] J. M. Martinis and M. Nahum, Phys. Rev. B **48**, 18 316 (1993).

[20] J. D. White and M. Wagner, Phys. Rev. B **48**, 2799 (1993).

[21] M. W. Keller, H. D. Jensen, and J. M. Martinis (unpublished).